JOURNAL OF Materials CHEMISTRY

Influence of the silica based matrix on the formation of iron oxide nanoparticles in the Fe_2O_3–SiO_2 system, obtained by sol–gel method

Andrei Jitianu,*[a] Maria Crisan,[a] Aurelia Meghea,[b] Ileana Rau[b] and Maria Zaharescu[a]

[a]*Institute of Physical Chemistry, Romanian Academy, 202 Splaiul Independentei, 77208 Bucharest, Romania. E-mail: ajitianu@chimfiz.icf.ro; Tel: 00 401 312 11 47*
[b]*''POLITEHNICA'' University of Bucharest, Romania, Faculty of Industrial Chemistry, 78126 Bucharest, Romania*

Received 20th November 2001, Accepted 6th February 2002
First published as an Advance Article on the web 21st March 2002

Composite iron oxide–SiO_2 materials were prepared by a sol–gel method starting with two types of precursors, tetraethoxysilane (TEOS) and methyltriethoxysilane (MTEOS), as the SiO_2 source. As the iron source a soluble Fe^{2+} salt, mainly $Fe(SO_4)_2 \cdot 7H_2O$, was used, the iron oxides were generated during the sol–gel process. The amorphous gels obtained were thermally treated up to 1000 °C in order to obtain iron oxides with different structures and grain size. The initial gels and the thermally treated samples were characterised by DTA/TGA analysis, DR-UV–VIS and IR-spectroscopy, EPR measurements, transmission electron microscopy (TEM) and BET surface area methods. The matrices obtained from the precursors play a major role in the evolution of the process. In both cases the initial gels are amorphous. In the non-porous matrix obtained by thermal treatment using methyltriethoxysilane (MTEOS), the tendency for crystallisation increases, and the iron oxide particle size is increased.

1 Introduction

The concept of nanomaterials first appeared in the last few decades, after investigation techniques were able to detect the small dimension of these kinds of materials. The ability to control the particle size and the morphology of the nanomaterials is of crucial importance nowadays both from the fundamental and industrial point of view.[1] The increasing interest in nanomaterials follows an excellent study published in 1986 by Smith,[2] which made a connection between physical properties and grain size of materials. Sol–gel oxide materials prepared in the Fe_2O_3–SiO_2 system may display specific magnetic, electrical, as well as catalytic properties both in bulk and in film forms. Using different methods, iron oxide nanoparticles in glass,[3] polymers,[4] LB films,[5] zeolites, clays[6] and mesoporous silicate[7] have been prepared. The first study on the Fe_2O_3–SiO_2 amorphous magnetic composite systems was accomplished by Yoshio *et al.*[8] in 1981.

Many studies on the iron oxides were designed to obtain γ-Fe_2O_3, which exhibits very important properties. Using the sol–gel method Tao *et al.*[9] prepared nanoparticles of γ-Fe_2O_3 in order to improve gas-sensing properties, together with a decrease in the particles' dimension.

In the same way, cermets in the Fe–SiO_2 system were obtained.[10–12] This kind of cermets could be obtained using *in situ* reduction by introduction of the reduction agent, for example glucose, in the sol–gel system.[10] Generally, the cermets are used in catalysis.[11,12]

γ-Fe_2O_3 (maghemite) embedded in SiO_2 has been carefully studied by Piccaluga *et al*,[13–17] since these nanocomposites present magnetic and catalytic applications. They obtained nanocomposites in the Fe_2O_3–SiO_2 system[13–17] and a structural characterisation of this kind of material has been carried out. Like Tao,[9] Cannas[17] used ethyleneglycol in the formation of γ-Fe_2O_3 in a SiO_2 matrix, which allowed the formation of metal oxide nanoparticles homogeneously dispersed over the amorphous silica matrix. The structural characterisation of the Fe_2O_3–SiO_2 system, which contained iron oxide between 9.1 and 33.2% wt., was realised by the following methods: EPR,[13,14] Moessbauer,[13] ^{29}Si-MAS-NMR and ^{1}H-NMR[15–17] and IR spectrometry.[15] The magnetic properties of these systems have also been characterised.[13,14]

Zhang *et al.*[18] have obtained magnetic single-domain γ-Fe_2O_3 super-paramagnetic nanoclusters in a sulfonated silica matrix. On the other hand, Morales *et al.*[19] carried out an interesting study on the magnetic properties of γ-Fe_2O_3 embedded in silica matrices obtained either by alkoxide or an aqueous route.

Other studies on the Fe_2O_3–SiO_2 system have been made by Lopez *et al.*[20,21] and in these studies some compositions contained iron between 0.1–15% wt. In one of these studies the thermal stability of nanocomposites was investigated,[21] in the other studies the structural evolution with temperature of this kind of nanocomposite was examined.[20]

In our previous papers[22–24] the preparation and characterisation of Fe_2O_3–SiO_2 nanocomposites have been achieved using three different methods:

1. The iron oxide was generated during the sol–gel process.
2. First the SiO_2 matrix was obtained, then the iron oxide was formed by precipitation of iron hydroxide inside the porous matrix after impregnation with a soluble Fe^{2+} salt and followed by thermal treatment.
3. Magnetite powder, prepared by wet chemical method, was mixed with a sol–gel solution, and was embedded in the SiO_2 based matrix after gelation.

Our previous studies[22–24] presented very heartening results for nanocomposites, with particle dimension in a desired range, when the iron oxides were generated during the sol–gel process. In the present work the influence of the matrix, obtained starting with TEOS and MTEOS respectively, on the structure and the size of the iron oxides nanoparticles was studied.

2 Experimental

Preparation of samples

All the samples were prepared in order to obtain nanocomposites with a final iron content of 3% wt. The gels were obtained

using the following reagents: tetraethoxysilane (TEOS) (Merck) and methyltriethoxysilane (MTEOS) (Merck) as SiO_2 source, and $FeSO_4 \cdot 7H_2O$ (Merck) as iron oxides source, absolute ethanol (Riedel de Haen) as solvent and deionized water for hydrolysis.

In Table 1 the composition of the starting solution and experimental conditions for the preparation of Fe_2O_3–SiO_2 nanocomposites, are presented.

Two solutions were prepared simultaneously: TEOS with ethanol and an aqueous solution of iron sulfate in which NH_4OH was introduced up to pH = 9. These two solutions were mixed together. The resulting solution was refluxed at 65 °C under constant stirring until gelation occurred. During the gelation process the pH of the reaction solution decreased up to values presented in Table 1. The samples were dried at 70 °C for 12 h.

According to the DTA/TGA results, the obtained gels were thermally treated for one hour at 200 °C, 550 °C and 1000 °C, respectively, using a heating rate of 1 °C min^{-1}.

Characterisation of samples

Thermodifferential (DTA) and thermogravimetric (TGA) analysis were carried out using MOM-Budapest OD-103 type Derivatograph in the temperature range of 20–1000 °C, with a heating rate of 10 °C min^{-1}.

IR spectra in the range 4000–200 cm^{-1} with a 4 cm^{-1} step were recorded using a Carl-Zeiss-Jena M80 type spectrometer using the KBr pellets technique.

Diffuse reflectance spectra (DR-UV–Vis) in the range 200–900 nm were recorded on a Varian Cary 4 spectrometer equipped with a Praying Mantis device, using self-supporting pellets. The diffuse reflectance spectra were also converted into absorption spectra with the Kubelka–Munk function $F(R_\infty)$[25] using $BaSO_4$ as a standard.

EPR spectra were recorded at room temperature using an ART-5-Bucharest spectrometer in X-band, with modulation of magnetic field 100 kHz.

The absorption capacity of these nanomaterials was controlled by nitrogen physisorption at 77 K using a Grimm BET automatic surface analyser.

For the estimation of the size of the Fe_2O_3 particles in the silica matrices, transmission electron micrographs were taken using a Phillips EM-420 using a LaB_6 cathode.

3 Results and discussions

From the data presented in Table 1 it is apparent that the alcohol–alkoxide ratios, as well as the gelling times, are different for the two samples. In the case of sample 2, a higher amount of ethanol was required in order to keep the miscibility of the solution up to the gelling point. Our previous work[23] with lower alcohol–alkoxide ratios showed that a separation of the initial homogeneous solutions into two immiscible liquids occurred resulting in di-phasic gels.

This phenomenon could be connected with the hydrophobic character of MTEOS due to the presence of methyl groups. The presence of the organic groups in the silica matrix could sterically hinder in part the formation of the Fe–O–Si bond. An increase in solvent quantity, slowed down the rate of hydrolysis–polycondensation processes and thus many –OH groups (hydrophilic area) became available to make connections with iron ions.

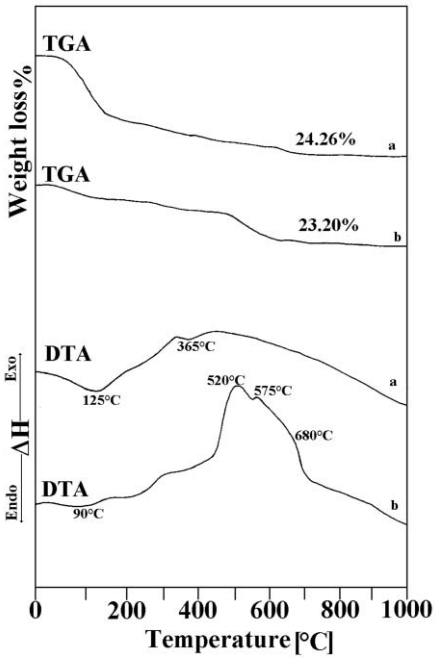

Fig. 1 DTA-TGA curves of systems Fe_2O_3–SiO_2 obtained with: a-TEOS, b-MTEOS.

In Fig. 1, the DTA-TGA curves are presented. The TGA curve of sample 1 presents two main steps of thermal decomposition between 20–195 °C and 195–770 °C, while the TGA curve of sample 2 presents three main steps of thermal decomposition between 20–140 °C, 140–425 °C and 425–725 °C. For both samples the first steps of thermal decomposition were found to be accompanied by endothermal effects, at 125 °C and 90 °C for sample 1 and sample 2, respectively. These effects were assigned to the desorbtion of water and ethanol adsorbed into the matrix.

The second step on the TGA curve of sample 1 was found to be accompanied by an endothermal effect at 365 °C. This effect was assigned to the evolution of the OH groups[21] and to the evolution of the unhydrolysable ethoxy moieties. The final step of thermal decomposition of sample 2 was found to be accompanied by three exothermal effects at 520 °C, 575 °C and 680 °C. The first two effects were assigned to the removal of the methyl groups from the matrix, and to the combustion of this organic part. The effect at 680 °C could be attributed to the re-organisation of the inorganic matrix after the removal of the organic component.

The thermal analysis showed that the main effects are due to the decomposition of the matrices. Since the concentration of iron used in the samples is low (3% wt.), the effects from the presence of the iron compounds in the matrix could not be detected because of overlap with the results from the matrix. It is known that the goethite (FeO(OH)) formed from sol–gel processes usually decompose at 340 ± 5 °C.[26]

The weight loss values of both samples were found to be similar. This could be explained by taking into account the

Table 1 Composition of the starting solution and experimental conditions for preparation of Fe_2O_3–SiO_2 nanocomposites

		Molar ratio					Conditions of reaction	
Samples	Precursors	EtOH/ alkoxide	H_2O/ alkoxide	Fe^{2+}/ alkoxide	NH_4OH/ alkoxide	pH	T/°C	t_{gel} /min
1	$FeSO_4 \cdot 7H_2O$ + TEOS	4	13.375	0.0325	0.0082	5.3	65	60
2	$FeSO_4 \cdot 7H_2O$ + MTEOS	8	13.375	0.0325	0.0082	4	65	180

different structure of the samples obtained with the two kinds of starting alkoxides. Therefore for the case of sample 1 the main weight loss was due to the removal of ethanol and water from the hydrophilic network. On the other hand for sample 2, the matrix is hydrophobic and the methyl groups close the pores of the matrix, so the quantity of water and ethanol from this sample is very low. Under this conditions, the main weight loss of the sample 2 was found to be due to the removal and burning of the methyl groups.

According to the DTA-TGA results, the samples were thermally treated as follows:

at 200 °C for removing water and organic moieties adsorbed on the matrices;

at 550 °C for removal of all the organic parts connected to the matrices;

at 1000 °C, in order to obtain a crystalline phase of iron oxides.

In Figs. 2 and 3 the IR spectra for the gels obtained starting with TEOS and MTEOS, before and after thermal treatment at 200 °C, 550 °C and 1000 °C, respectively are presented. All spectra of sample 1 (Fig. 2) present the main vibrations characteristic for silica network reported by Bertoluzza *et al.*[27] In the IR spectrum of the fresh sample, the very characteristic bands ν_{as}(Si–O–Si) at 1196 cm^{-1} and 1085 cm^{-1}, respectively, were found. In the case of the sample treated at 550 °C, the shoulder from 1196 cm^{-1} is shifted to 1213 cm^{-1}. At 1000 °C, this shoulder was found to be very weak and shifted to 1220 cm^{-1}. The characteristic ν_s(Si–O(H)) vibration at 940 cm^{-1} was found in the IR spectra of the uncalcined sample. This band decreased with temperature, so after the calcination at 1000 °C, it disappeared. The decrease in intensity and disappearance of signals could be connected with the increase of intensity of the band assigned to ν_s(Si–O–Si) at 794 cm^{-1}. Therefore, the silica matrix becomes more structurally ordered as the temperature increases. In the literature studies, there is some debate concerning the shoulder at 571 cm^{-1}. Some authors consider that the shoulder could be due to the defects arising from broken bonds,[28] others consider that the band occurs from the surface of polycrystalline clusters[29] however, most authors consider that this band could be assigned to a specific vibration due to the presence of cyclic tetramers.[30] The last supposition was taken into account in this paper. The band characteristic for the cyclic tetramers disappears when the sample is heated at 1000 °C, because the cyclic tetramers are not stable at this temperature. The shoulder at 590 cm^{-1} has been assigned by Bruni *et al.*[15] to the stretching vibration νFe–O which in our case was covered by the band of silica cyclic tetramers. The bending vibration of O–Si–O group was detected at 458 cm^{-1}, for the fresh samples, and for the samples heated at 200 °C and 550 °C. In the case of the sample heated at 1000 °C this peak was shifted to 467 cm^{-1}. This shift could be assigned to the crystallisation of α-Fe_2O_3, it has been proposed[20,31] that in the spectral region 500–400 cm^{-1} a characteristic vibration for νFe–O occurs.

The characteristic band for stretching (OH) groups was found around 3400 cm^{-1} in all samples. The band at 1637 cm^{-1} was assigned to the bending vibration of water molecules δ(HOH). Only in the case of IR spectra of the fresh sample, was a weak shoulder at 1357 cm^{-1} observed. After the thermal treatment this peak vanished and was assigned to the symmetric bending vibration (δ_s(CH)) of the C–H bond. The δ_s(CH) vibration was found to belong to the ethoxy groups from the un-reacted alkoxide.[20]

As observed from Fig. 2, the IR spectra of the initial gels and the sample thermally treated at 200 °C and 550 °C are very similar. The important differences appeared after thermal treatment at 1000 °C. Up to 550 °C for sample 1, the main effect was removal of the water molecules and organic groups followed by the reorganisation of the matrix.

In Fig. 3 the IR spectra of sample 2 are presented. The IR spectra of this sample show, besides the vibrational band characteristic for silica matrices, the structural bands characteristic for the ≡Si–C bonds. There were no notable differences between the fresh sample and that heated at 200 °C.[32,33]

In the case of fresh samples and samples calcined at 200 °C, a band at 2989 cm^{-1} assigned to $\nu_{as}(CH_3)$ was found. The two bands at 1425 cm^{-1} and 1286 cm^{-1}, respectively, were assigned to the symmetric and asymmetric bending vibration of the C–H bond from the CH_3 groups bonded at silicon atom. Two other peaks were observed at 899 and 904 cm^{-1}. These peaks were assigned to the vibrational band ρ (CH_3). On the other hand, the new band that appeared at 676 cm^{-1} in the IR spectra of fresh sample 2, was assigned to a symmetric stretching vibration of the C–Si bond. At 550 °C and 1000 °C, the bands assigned to the presence of methyl groups connected to silicon atoms disappeared since the CH_3 groups from the silica matrix were eliminated.

Capozzi *et al.*[32,33] and Bertoluzza *et al*[27] assigned the IR bands at 1130 cm^{-1} and 1020 cm^{-1} of fresh sample and sample

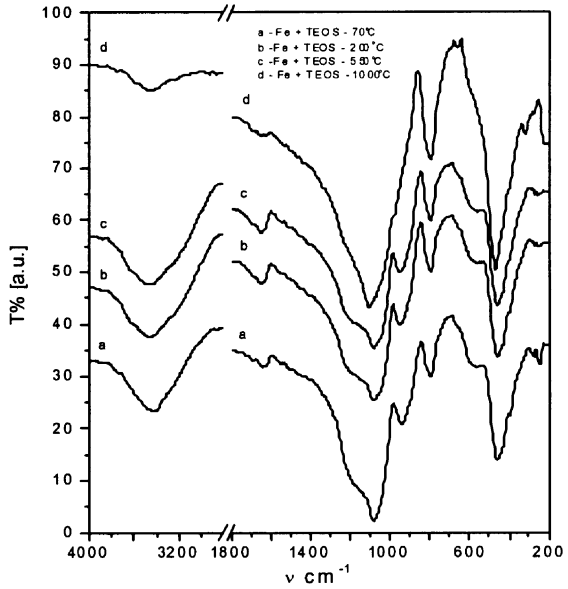

Fig. 2 IR spectra of nanocomposites Fe_2O_3–SiO_2 obtained from TEOS at different temperatures.

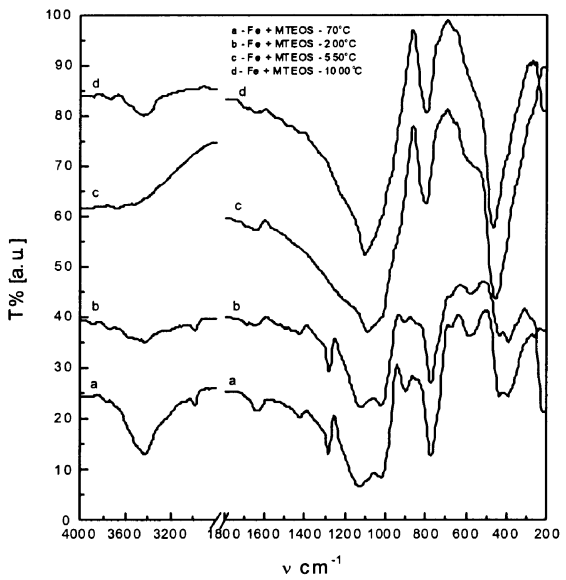

Fig. 3 IR spectra of nanocomposites Fe_2O_3–SiO_2 obtained from MTEOS at different temperatures.

treated at 200 °C to a ν_{as}(Si–O–Si) vibration characteristic for LO mode and TO mode, respectively. At 550 °C, these bands are not very well defined, but the tendency is to become similar to the spectrum of the material prepared starting with TEOS. The same pattern of peaks was obtained with samples treated at 1000 °C and the bands were identified at 1220 cm^{-1} as a shoulder, and at 1080 cm^{-1}.

For sample 2 treated at lower temperature, 200 °C and fresh sample, the characteristic band for ν_s(Si–O–Si) was shifted to lower energy (724 cm^{-1}) with respect to the sample treated at 550 °C, (804 cm^{-1}) and 1000 °C (799 cm^{-1}). This shift was attributed to an overlap of this vibration with the vibration of ν_s(C–Si).[32,33] The characteristic band for the δ(O–Si–O) vibration was distorted before the removal of the organic part. The band at 575 cm^{-1}, was assigned to the presence of cyclic tetramers, compare with sample 1. In this spectral range Bruni *et al*[15] also found the ν(Fe–O) vibration. None of the IR spectra of sample 2 showed the characteristic vibrations of ν(Si–O(H)) at 970 cm^{-1}. This could be connected with the hydrophobic character of MTEOS.

For all samples, a peak at 3420 cm^{-1} characteristic for the νOH vibrations appeared in the IR spectra. In all IR spectra, the characteristic band for the bending vibration of water molecules was found at 1638 cm^{-1}.

The IR spectra of samples 1 and 2 treated at 1000 °C did not have any important differences. Therefore it could be concluded, that after thermal treatment at 1000 °C the structure of the samples is similar.

In Figs. 4 and 5 the DR/UV–VIS spectra of Fe_2O_3–SiO_2 nano-materials obtained with TEOS and MTEOS, respectively, are presented, for the fresh and calcined samples. In the fresh samples the iron ion is in the three-oxidation state and have a d^5 configuration. The ground state configuration for Fe(III) is $[t_{2g}(xy,xz,yz)]^5$ for a low spin, and the corresponding spectroscopic term is T_{2g}. The spin-orbit coupling coefficient for Fe(III) is too small for inter-configuration transitions to be observed.[34]

The UV–VIS spectra of Fe(III) ion in octahedral surroundings show in general the following d–d transitions,[34] according to Tanabe–Sugano diagram:

$^2T_{2g} \rightarrow {}^4T_{1g}$ (spin forbidden)

$^2T_{2g} \rightarrow {}^4T_{2g}$ (spin forbidden)

$^2T_{2g} \rightarrow {}^2A_{2g}$, $^2T_{1g}$ (spin allowed)

$^2T_{2g} \rightarrow {}^2E_g$ (spin allowed)

As observed from Fig. 4, all spectra of sample 1 up to 550 °C present a charge transfer (CT) band at 218 nm. This CT band was assigned to the electron transfer from the free electron pair of the oxygen atom (from water and OH groups) to the t_{2g}, e_g empty iron ion orbitals. In the case of the fresh sample (Fig. 4),

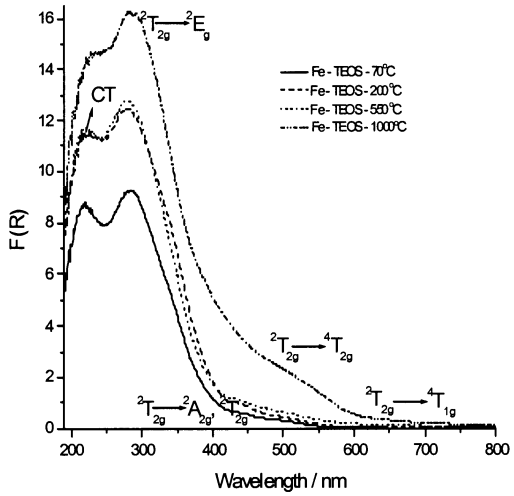

Fig. 4 DR/UV–VIS spectra of nanocomposites Fe_2O_3–SiO_2 obtained from TEOS at different temperatures.

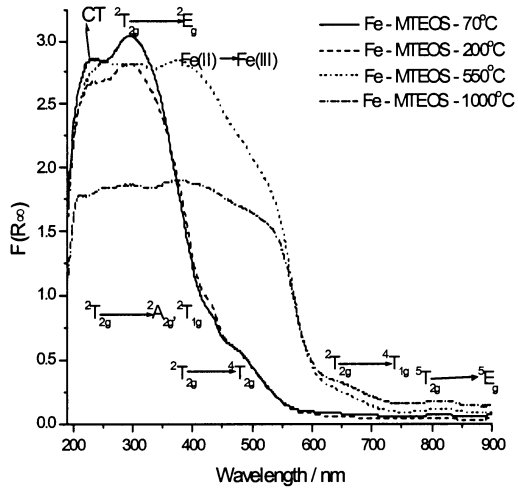

Fig. 5 DR/UV–VIS spectra of nanocomposites Fe_2O_3–SiO_2 obtained from MTEOS at different temperatures.

this band is very distinct. After heat treatment up to 550 °C, this band decreased with respect to the band at 289 nm. This decrease could be connected with the removal of the water molecules and part of the OH groups. At 1000 °C, this band was shifted to low energy and it was present like a shoulder. The presence of this band at this temperature could be connected with the presence of the residual OH groups. Some authors[20] consider that the band at 283 nm in the UV–VIS spectra of the fresh sample is due to another CT band, formed from the presence of the sulfate ions. In contrast, other authors[34] consider that this band is due to the d–d transfer to the ^2E_g.

The presence of two large charge transfer bands hinder the d–d bands which therefore have a lower intensity. Because the band at 283 nm for the fresh sample increased in intensity after the thermal treatment up to 1000 °C, it was concluded that in addition to the CT bands due to the presence of SO_4^{2-} ions, a d–d transfer band $^2T_{2g} \rightarrow {}^2E_g$exists. For all spectra of sample 1, an absorption band around 430 nm was present. This band appears in all cases, in the fresh sample at 430 nm, but shifted to 439 nm for the sample treated at 200 °C, at 445 nm for the sample treated at 550 °C and at 460 nm for the sample treated at 1000 °C, but it is a very large shoulder in the last case. This band could be assigned to a d–d transition to ($^2A_{2g}$, $^2T_{1g}$). In the case of sample 1 treated at 1000 °C, a very distinct band at 525 nm appeared. This band was detected to a lesser extent in the samples treated at lower temperatures, and was assigned to a d–d spin forbidden transfer to $^4T_{2g}$. In the UV–VIS spectra of sample 1 thermally treated at 550 °C and 1000 °C, a band due to another spin forbidden transition to $^4T_{1g}$ around 650 nm was observed.

The d–d bands from all DR/UV–VIS (Fig. 4) spectra of sample 1 were found to be characteristic for an iron ion in an octahedral surrounding. Lopez *et al*.[20] showed that iron oxides in a silica matrix are involved in the polymeric chains as shown below.

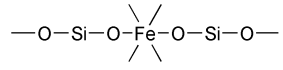

This study evidenced that the iron is embedded in the same type of polymeric chains both for the fresh gel and for those treated at lower temperatures.

Fig. 5 presents the UV–VIS spectra of sample 2, fresh and after thermal treatment at 200 °C, 550 °C and 1000 °C, respectively. The spectra of the fresh sample 2 and sample treated at 200 °C present approximately the same bands and

trend, as those for sample 1. The CT bands due to the presence of water were recorded at 230 nm and they decreased in intensity with the increase in temperature. The band at 290 nm present in the spectra of fresh sample and sample treated at 200 °C, was assigned both to a CT band and a d–d transfer to ^2E_g.[34] The band assigned to a d–d transition ($^2A_{2g}$, $^2T_{1g}$) was detected at 431 nm in the UV–VIS spectra of fresh sample 2 and also for the sample treated at 200 °C. The forbidden spin transfer to $^4T_{2g}$ was detected in the spectra of this sample at 487 nm. In comparison with sample 1, this band is shifted to higher energy. The same situation was observed for the band assigned to a spin forbidden transfer to $^4T_{1g}$ which presented a blue shift with respect to the materials obtained with TEOS. This shift could be connected with the presence of $-CH_3$ groups in the matrix. In this case some of the iron ions were involved in the chains –O–Si–O–Fe–O–Si–O– as for the case of materials prepared with TEOS. Since, the methyl groups were present in the inorganic matrix, they blocked one site of the silicon atoms. Other iron ions, which were not involved in polymer chains, could form nanoclusters on the surface of materials. This separation of nano-clusters could be connected to the hydrophobic character of the matrix obtained with MTEOS and/or steric hindrance occurring due to the presence of methyl groups in the matrix. After heating sample 2 at 550 °C, the main CT band at 230 nm remained unchanged, but the band at 297 nm in the spectra of fresh sample was shifted to 313 nm. The main difference appeared in the visible region, where new bands appeared at 376 nm and at 821 nm. The first band at 376 nm was assigned to the d–d transfer between Fe(II) → Fe(III). The presence of Fe(II) was evidenced by the appearance of the band at 821 nm which was assigned to $^5T_{2g} \rightarrow {}^5E_g$ for Fe(II). The presence of Fe(II) could be explained by the partial reduction of Fe(III) during the burning of the organic moieties, which forms a reducing atmosphere. After heating at 1000 °C, the bands in the UV–VIS spectra of sample 2 decreased in intensity, but were the same as for the sample treated at 550 °C.

The UV–VIS spectra for both samples at all temperatures are characteristic of iron ions in an octahedral surrounding.

In Figs. 6 and 7 the EPR spectra of samples 1 and 2, respectively, are presented. In the case of gels obtained from TEOS treated at 200 °C and 550 °C the EPR spectra showed two main signals at $g \sim 2$ and $g \sim 4.3$, which could be assigned to two different Fe(III) sites.[35,36] Both signals at $g \sim 2$ and $g \sim 4.3$ were observed for EPR spectra of the sample 1 thermally treated at 200 °C and 550 °C and for sample 2 treated at 200 °C. The broad resonance at $g \sim 2$ was assigned to a strong

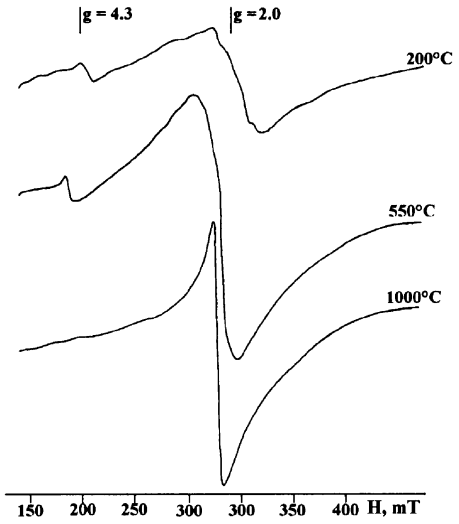

Fig. 6 EPR spectra of nanocomposite system Fe_2O_3–SiO_2 obtained from TEOS at different temperatures.

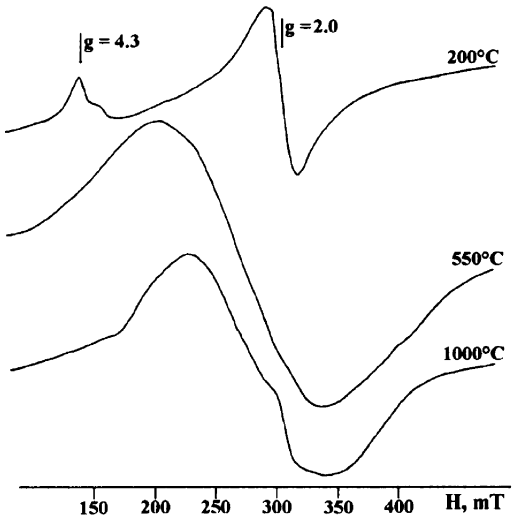

Fig. 7 EPR spectra of nanocomposite system Fe_2O_3–SiO_2 obtained from MTEOS at different temperatures.

interaction between Fe(III) ions in octahedral sites and the bulk material. This band could be assigned to the iron from the chain: –O–Si–O–Fe–O–Si–O–. In the case of compound calcined at 200 °C, this band was observed at a lower intensity, this could be connected to the lower degree of crystallinity and with a structural disorder of the material obtained at this temperature. The second signal with $g \sim 4.3$ corresponds either to strongly distorted orthorhombic sites located on the surface or to the isolated Fe(III) ions dispersed in the silica matrix.[14] In the case of the samples obtained with TEOS, the ratio of the signal intensity at $g \sim 4.3$ to that at $g \sim 2$ decreased with an increase in temperature of thermal treatment. In the case of sample treated at 1000 °C, the EPR spectrum presented a high symmetric peak located at $g = 2$. This band could be assigned to a super-paramagnetic material. Tanaka *et al.*[36] observed that Fe(III) ions in spin pair of Fe^{3+}–O^{2-}–Fe^{3+} also can give a strong and very symmetric signal at $g \sim 2$. This observation could be connected with the formation of α-Fe_2O_3 at 1000 °C in this system by breaking the chain –O–Si–O–Fe–O–Si–O–. On the other hand, this band could be assigned to the small dimension of the particles of the iron oxide present in this material.

In the case of the materials 2, the EPR spectra of the sample treated at 200 °C presented two signals, as for the case of samples 1 at the same temperature. In the case of sample treated at 550 °C, this gave an EPR spectrum characteristic for ferromagnetic materials. This ferromagnetic character could be obtained by a partial reduction of Fe(III) ions to Fe(II) ions during burning out of the organic moieties, which form a reducing atmosphere. The Fe(II) ions usually do not give any EPR signal, but the presence of these ions could influence the signal of Fe (III) ions.

The sample treated at 1000 °C also gave an EPR spectrum characteristic of a ferromagnetic material, with an asymmetric broader band, with respect to the spectrum of the sample treated at 550 °C. This behaviour was correlated with the start of crystallisation of α-Fe_2O_3 nano-particles in the silica matrix.

The textural characteristics of the samples, obtained from

Table 2 Textural characteristics of the samples

Sample	Temperature/°C	BET surface area/m^2g^{-1}	*d*/nm
1	200	63	Amorphous
	550	72	Amorphous
	1000	<1	9–19
2	200	<1	22–37
	550	15	38–47
	1000	<1	37–51

the BET and TEM measurements, are presented in Table 2. The TEM micrographs of the samples 1 and 2 are presented in Figs. 8 and 9, respectively.

As observed from Table 2, the BET surface area increased in both cases after the thermal treatment at 550 °C. This increase could be connected with the removal of the organic moieties present in the matrix. In the case of materials obtained starting with TEOS, the organic moieties were ethanol and unreacted ethoxy groups. For the materials obtained with MTEOS, the BET surface increased after the sample was treated at 550 °C by removal and burning of chemically bonded methyl and unhydrolysable groups. In the case of samples from MTEOS, materials with a lower porosity were obtained. In the first step of the thermal treatment, the presence of the methyl groups in the pores of the sample could explain the low BET surface area. After heating the sample at 550 °C and 1000 °C, respectively,

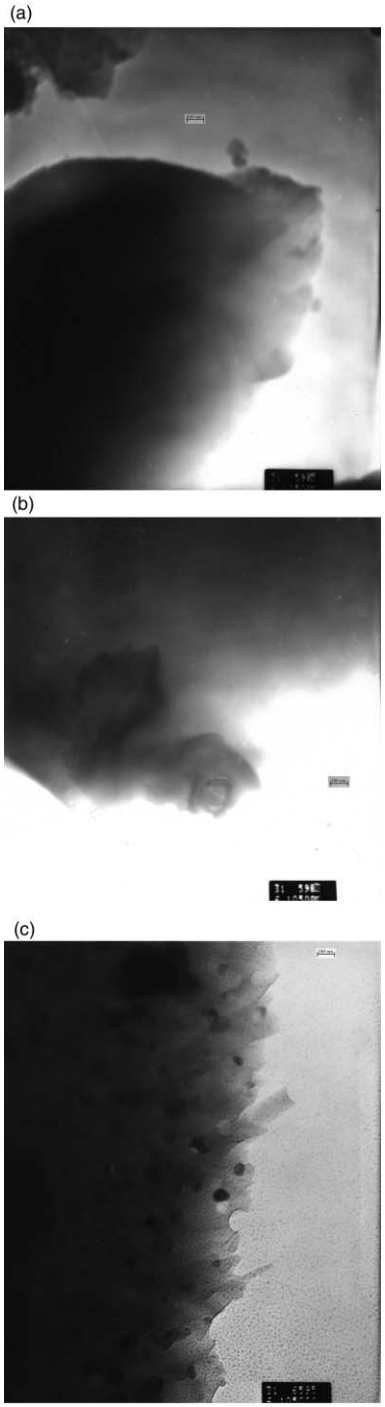

Fig. 8 TEM micrographs of system Fe_2O_3–SiO_2 obtained from TEOS at: a 200 °C; b 550 °C; c 1000 °C.

Fig. 9 TEM micrographs of system Fe_2O_3–SiO_2 obtained from MTEOS at: a 200 °C; b 550 °C; c 1000 °C.

the lower values of the surface area with respect to the samples obtained with TEOS, could be explained by the collapsing of the structure after the removal of the methyl groups. After the removal of these groups, the silicon atom had the tendency to regain its characteristic coordination number, which is usually 4.

The TEM micrographs for the sample 1 treated at 200 °C (Fig. 8a) and 550 °C (Fig. 8b) respectively, prepared starting with TEOS, presented only a dark field. In this field at this magnification it was not possible to observe distinct particles of iron oxide. This dark field is usually observed for amorphous materials. This observation confirms the presence of the polymeric chain –O–Si–O–Fe–O–Si–O–, since the iron oxide particles could not be seen because the iron ions are bonded in the chain.

In the case of sample treated at 1000 °C (Fig. 8c) it was possible to observe particles of Fe_2O_3 with dimensions in the range 9–19 nm. These particles appear after the –O–Si–O–Fe–O–Si–O– chain was broken at this temperature and α-Fe_2O_3 crystallised.[24]

In the case of TEM micrographs of sample 2 it can be observed that nanoclusters as aggregates appeared already at 200 °C (Fig. 9a). These nanoclusters appear because this kind of matrix has a hydrophobic character. Besides a dark field due to the amorphous part of the samples, nanoclusters aggregates could be observed, from 200 °C. In this case not all iron ions were connected in –O–Si–O–Fe–O–Si–O– bonds. The iron ions, which were not involved in polymer chains, were isolated either in the hydrophobic part of the matrix and created iron oxide nanoclusters, or on the surface where they were able to make clusters. In the micrographs in Fig. 9a, a dark field is observed, and this is assigned to the amorphous part of the sample. In the case of the sample treated at 550 °C (Fig. 9b) the dark field was more extended. This could be explained because at this temperature the system reorganises after the removal of the methyl groups from the matrix. In the case of the sample treated at 1000 °C (Fig. 9c), Fe_2O_3 nanoclusters crystallised.

The dimension of particles in the Fe_2O_3–SiO_2 system obtained with MTEOS did not increase so much from the sample treated at 200 °C to the sample treated at 1000 °C, as it could be observed in Table 2. This fact could be explained by the influence of the matrix, which hinders the increasing of the dimension of particles, under the constraints imposed by the matrix.

4 Conclusion

Nanocomposites in the Fe_2O_3–SiO_2 systems were obtained using the sol–gel method. Two kinds of alkoxides were used for obtaining the silica matrix: tetraethoxysilane (TEOS) and an organic modified alkoxide methyltriethoxysilane (MTEOS).

The influence of the matrix obtained from the TEOS and MTEOS precursor plays a major role in the evolution of the process. In both cases the initial gels were amorphous.

The study also made the connection between structural evolution after heating and the thermal stability of the materials.

The main difference between the materials obtained starting with TEOS and MTEOS was the temperature where the formation of Fe_2O_3 could be observed. In the case of the materials started from TEOS the iron oxide nanoparticles were observed at 1000 °C, while for the nanocomposites obtained from MTEOS the same nano-clusters were visible already in the materials thermally treated at 200 °C.

In the case of the materials obtained by thermal treatment using methyltriethoxysilane (MTEOS), the tendency of crystallisation of iron oxides increases. The iron oxide particle size did not increase significantly after thermal treatment from 200 °C to 1000 °C. This fact could be explained by effects of the hydrophobic matrix. The hydrophobic character of MTEOS-based matrix determined the concentration of the hydrophilic iron based nano-clusters on the surface of the gel.

For materials obtained by thermal treatment using tetraethoxysilane (TEOS), the tendency of crystallisation did not appear up to 550 °C because the iron ions were bonded in the chains:–O–Si–O–Fe–O–Si–O–. After thermal treatment at 1000 °C, these chains were broken and α-Fe_2O_3 crystallised.

References

1 L. Vayssieres, A. Hagfeldt and S. E. Lindquist, *Pure Appl. Chem.*, 2000, **72**, 47.
2 W. F. Smith, *Principles of Materials Science Engineering*, MacGraw Hill Book Company, Singapore 1986, p. 128.
3 N. F. Borrelli, D. W. Hall, H. J. Holland and D. W. Smith, *J. Appl. Phys.*, 1987, **61**, 5399.
4 Y. Wang, A. Suna, W. Mahler and R. Kasowski, *J. Chem. Phys.*, 1987, **87**, 7315.
5 Y. Tian, C. Wu and J. H. Fendler, *J. Phys. Chem.*, 1984, **98**, 4913.
6 A. Jentys, R. W. Grimes, J. D. Gale and C. R. A. Catlow, *J. Phys. Chem.*, 1993, **97**, 13535.
7 T. Abe, Y. Tachibana, T. Uematsu and M. Iwamoto, *J. Chem. Soc., Chem. Commun.*, 1995, 1617.
8 T. Yoshio, C. Kawaguchi, F. Kanamaru and K. Takahashi, *J. Non-Cryst. Solids*, 1981, **43**, 129.
9 S. Tao, X. Liu, X. Chu and Y. Shen, *Sens. Actuators*, 1999, **B61**, 33.
10 A. Basumallick, K. Biswas, S. Mukherjee and G. C. Das, *Mater. Lett.*, 1997, **30**, 363.
11 S. Tanabe, T. Ida, M. Suginava, A. Ueno, Y. Katera, K. Toheje and Y. Udagawa, *Chem. Lett.*, 1984, 1567.
12 T. Akuyama, E. Tanigawa, T. Ida, H. Tsuiki and A. Ueno, *Chem. Lett.*, 1986, 723.
13 G. Ennas, A. Masinu, G. Piccaluga, D. Zedda, D. Gatteschi, C. Sangregorio, J. L. Stanger, G. Concas and C. Spano, *Chem. Mater.*, 1998, **10**, 495.
14 C. Cannas, D. Gatteschi, A. Masinu, G. Piccaluga and C. Sangregorio, *J. Phys. Chem. B*, 1998, **102**, 7721.
15 S. Bruni, F. Cariati, M. Casu, A. Lai, A. Musinu, G. Piccaluga and S. Solinas, *Nanostruct. Mater.*, 1999, **11**, 573.
16 M. Casu, F. C. Marincola, A. Lai, A. Masinu and G. Piccaluga, *J. Non-Cryst. Solids*, 1998, **232–234**, 329.
17 C. Cannas, A. Masinu and G. Piccaluga, *J. Sol–Gel Sci. Technol.*, in the press.
18 L. Zhang, G. C. Papefthymiou, R. F. Ziolo and J. Y. Ying, *Nanostruct Mater.*, 1997, **9**, 185.
19 M. P. Morales, M. J. Munoz-Aguado, J. L. Garcia-Placios, F. J. Lazaro and C. J. Serna, *J. Magn. Magn. Mater.*, 1998, **183**, 232.
20 T. Lopez, J. Mendez, T. Zamudio and M. Villa, *Mater. Chem. Phys.*, 1992, **30**, 161.
21 T. Lopez, J. Mendez-Vivar and M. Asomoza, *Thermochim. Acta*, 1993, **216**, 279.
22 M. Zaharescu, M. Crisan, A. Jitianu and D. Crisan, *Chem. Bull. "Politeh." Univ. Timisoara*, 1999, **44**, 53.
23 M. Zaharescu, M. Crisan, A. Jitianu, D. Crisan, A. Meghea and I. Rau, *J. Sol-Gel Sci. Technol.*, 2000, **19**, 631.
24 I. Peleanu, M. Zaharescu, I. Rau, M. Crisan, A. Jitianu and A. Meghea, *J. Radioanal. Nucl. Chem.*, 2000, **246**, 557.
25 P. Kubelka and F. Munk, *Z. Tech. Phys.*, 1931, **12**, 593.
26 C. Duval, *Inorganic Thermogravimetric Analysis*, 2nd edn., Elsevier, Amsterdam, 1963, p. 325.
27 A. Bertoluzza, C. Fagnano and M. A. Morelli, *J. Non-Cryst. Solids*, 1982, **48**, 117.
28 R. H. Stolen and G. E. Walrafen, *J. Chem. Phys.*, 1976, **64**, 2623.
29 C. J. Philipps, *J. Non-Cryst. Solids*, 1984, **63**, 347.
30 H. Yoshima, K. Kaniga and H. Nasu, *J. Non-Cryst. Solids*, 1990, **126**, 68.
31 E. N. Iurchenko, G. N. Kustova and C. C. Bachanov, *Kolebatelnie Spectri Neorganicheskih Soedinenii*, Izdatelstvo "Nauka", Novosibirsk, 1981, p. 52 (Russian).
32 C. A. Capozzi, L. D. Pye and R. A. Condrate Sr., *Mater. Lett.*, 1992, **15**, 130.
33 C. A. Capozzi, R. A. Condrate Sr., L. D. Pye and R. P. Hapanowicz, *Mater. Lett.*, 1992, **15**, 233.
34 A. B. P. Lever, *Inorganic Electronic Spectroscopy*, Elsevier, Amsterdam, 1984, pp. 453–459.
35 C. Craciun and A. Meghea, *Clays Clay Miner.*, 1985, **20**, 423.
36 K. Tanaka, K. Kamiya, M. Matsuoka and T. Yoko, *J. Non-Cryst. Solids*, 1987, **94**, 365.